Catalytic Antioxidant Activity of Two Diterpenoid Polyphenols of Rosemary, Carnosol and Isorosmanol, against Lipid Oxidation in the Presence of Cysteine Thiol

Hayate Higashino, Asuka Karatsu, and Toshiya Masuda*

Graduate School of Human Life Science, Osaka Metropolitan University, Sumiyoshi, Osaka 558-8585, Japan

*Corresponding Author

ABSTRACT:

Lamiaceae herbs such as rosemary have excellent antioxidant properties, and lipidic diterpenoid constituents, such as carnosol, are known as characteristic components to exhibit strong antioxidant activity. This study investigates the effect of thiol compounds on the antioxidant properties of diterpenoid polyphenols. The results concerning the antioxidant activity of polyphenols in the presence of thiol showed that two polyphenols, namely carnosol and isorosmanol, enhanced antioxidant capacity against the radical-induced oxidation of lipids. Further examination of the mechanism revealed that both polyphenols exhibit excellent catalytic antioxidant activity by using the thiol group as a reduction source. Using density functional theory calculations, we attempted to explain why only these two polyphenols exhibit catalytic antioxidant properties. The calculation results and the assumed reaction mechanism suggested that the orthoquinones produced in the antioxidant reactions of carnosol and isorosmanol are more unstable than the others, and that the regioselectivity of their reactions with thiols contributes to their catalytic antioxidant properties.

KEYWORDS: *Carnosol, Isorosmanol, Catalytic Antioxidant, Rosemary, Cysteine Thiol*

INTRODUCTION

The addition of antioxidants is one of the best ways to prevent the oxidative deterioration of foods. Therefore, the development of effective antioxidants, both artificial and natural, has been underway in recent years. However, these antioxidants are not always as effective when used in actual food products.[1] Of the many possible reasons for this, one is that foods are complex systems consisting of various ingredients. For example, effect varies in of emulsion-based foods depending on whether the antioxidant is in the aqueous or oil phase, as well as its presence at the interface, which can explain the so-called polar paradox phenomenon.[2] The coexistence of antioxidants is known to affect the total antioxidant capacity. The antioxidant effects of coexisting substances have been reported to add up in effects, however, synergistic and antagonistic effects have also been observed.[3,4] To better understand the function of antioxidants, an analysis is necessary, assuming the influence of other components in food. If the resulting synergistic effects could enhance the function of existing antioxidants, technologies could in turn be developed to prevent the oxidative degradation of foods more effectively and for longer with the addition of smaller amounts.

Lamiaceae herbs, such as rosemary and sage, are known to have particularly strong

antioxidant properties.[5] This can be attributed to lipid-soluble abietane diterpenoid polyphenols, such as carnosol, as well as water-soluble rosmarinic acid. A lipidic rosemary extract, which contains carnosol and related diterpenes, has a high radical-scavenging antioxidant capacity, especially against lipid oxidation.[6] Furthermore, it has been reported to have synergistic effects with other antioxidants,[7] although the mechanism is not fully understood. Our recent research examines the interactions of carnosol and related diterpenoid polyphenols [carnosic acid (**CA**), carnosol (**CAR**), rosmanol (**ROS**), isorosmanol (**isoROS**), and epirosmanol (**epiROS**)] isolated from rosemary with other food components. The current paper reports the results of studies on the enhancement of the antioxidant function and its mechanism in the presence of a thiol compound as a model cysteine-containing food ingredient.

MATERIALS AND METHODS

Chemicals and Instruments. 2,2′-Azobis(2,4-dimethylvaleronitrile) (AMVN) was purchased from FUJIFILM Wako (Osaka, Japan). Ethyl linoleate was purchased from Kanto Chemical (Tokyo, Japan) and utilized after purification using Florisil (FUJIFILM Wako) eluted with hexane.[8] A mixture of ethyl linoleate hydroperoxide isomers was obtained through the air oxidation of ethyl linoleate according to the method described

by Terao and Matsushita.[9] *N*-Benzoylcysteine methyl ester (**BCysM**) and *N,N′*-dibenzoylcystine dimethyl ester [**(BCysM)²**] were synthetically prepared using the previously reported method.[10] The organic solvent extract of rosemary prepared of rosemary leaves was provided by Mitsubishi Chemicals (Yokohama, Japan). Carnosol (**CAR**) and carnosic acid (**CA**) as well as the quinone derivative of **CAR** (**CARQ**) were prepared according to the reported methods.[11,12] All solvents and other reagents of extra pure or high-performance liquid chromatography (HPLC) grade were obtained from Nacalai Tesque (Kyoto, Japan). Nuclear magnetic resonance (NMR) spectra were recorded on a JNM-ECZ400S spectrometer (400 MHz; JEOL, Tokyo, Japan), while mass (MS) spectra were recorded on a JMS-T100 spectrometer (JEOL) using direct analysis in real-time (DART) and time-of-flight measurement modes. The molecular formulas of the compounds were obtained from high-resolution mass spectrometry (HR-MS) data using ChemCalc.[13] Analytical HPLC was performed on the reaction products using a PU-4180 quaternary gradient pump (JASCO, Tokyo, Japan) equipped with an MD-4015 photodiode array detector (JASCO). The data were analyzed using ChromNAV software (ver.1.19.02, JASCO). The HPLC system used for lipid peroxide analysis consisted of an LC-10AD pump and an SPD-10Avp UV detector (Shimadzu, Kyoto, Japan). The obtained data were analyzed using ChromNavi Lite (v.2.04.00,

JASCO). Preparative HPLC was performed using an LC-6AD pump (Shimadzu) equipped with an SPD-6A UV detector (Shimadzu).

Preparation of ROS, isoROS, and epiROS. A lipidic extract of rosemary (50 g) was subjected to octadecylsilyl silica gel (ODS) column chromatography (1 kg of Cosmosil 140C18-OPN, Nacalai Tesque) eluted step gradient from 50%, 60%, and 70% methanol in H_2O (2 L each) to obtain three fractions (0.46 g, 1.15 g, and 1.62 g) containing **isoROS**, **ROS**, and **epiROS**. These fractions were purified by HPLC using a Cosmosil 5C18-AR-II column (250 × 20 mm i.d.) and 1% acetic acid in H_2O–CH_3CN (55:45) as the solvent (flow rate = 20 mL/min; detection wavelength = 284 nm) to yield pure **isoROS** (250 mg), **ROS** (630 mg), and **epiROS** (350 mg). The isolated compounds were identified by comparison of their HR-MS and ^{1}H-NMR data with reported them.[14–16] (Analytical data for structure identification can be found in Supporting Information)

Measurement of the antioxidant activity of rosemary polyphenols with and without thiol (BCysM). To 34 μL of ethyl linoleate in a 10 mL screw-capped tube (1.6 mm i.d.× 100 mm h), added 4 mM rosemary polyphenol in acetone (63 μL), 0.3 M AMVN in CH_3CN (100 μL, CH_3CN), and 4 mM **BCysM** in acetone (0, 63, 126, or 189 μL) were successively added. The volume of the solution was adjusted to 2 mL with CH_3CN. The solution was then incubated at 37°C by shaking (100 min^{-1}) in the dark

using a water-bath shaker. A 20 μL aliquot was removed from the solution at 1-h intervals, and diluted with 380 μL of methanol. Ten microliters of the diluted solution were injected into the HPLC system to analyze the ethyl linoleate hydroperoxides under the following conditions: column, YMC-ODS-A (150 × 4.6 mm i.d.) (YMC, Kyoto, Japan); solvent, CH_3CN/H_2O (9:1, v/v); flow rate,1.0 mL/min; and detection, 234 nm. The concentration of hydroperoxides was calculated from the peak area of *trans, trans*-2,4-hexadien-1-ol as the alternative compound using the following calibration equation. y = 588,093x + 44,187 [y, peak area at 234 nm; x, amount (nmol) of *trans, trans*-2,4-hexadien-1-ol (range, 0.1–10 nmol)]

Analysis of the reaction products from CAR in the antioxidant reaction with and without thiol (BCysM). The reaction solution of **CAR** with and without **BCysM** (one molar equivalent), were prepared using the same procedure described above. At the same intervals, an additional 10 μL aliquot was removed from the reaction solution and injected into the HPLC system to analyze the reaction products using the following conditions: column, Cosmosil 5C18-AR-II (250 × 4.6 mm i.d, Nacalai Tesque); solvent A, acetic acid–H_2O (1:100); solvent B, CH_3OH; gradient conditions, B% (time) = 60% (0 min), 100% (40 min), and 100% (40–50 min); flow rate flow rate, 0.5 mL/min; and detection, 245 and 284 nm. The concentration of observed compound was calculated

from the peak area using the following calibration equations: **BCysM**: y = 486,771x + 192,287 [y, peak area at 245 nm; x, amount (nmol) (range, 0.1–50 nmol); **(BCysM)^2**: y = 1,097,523x + 9631 [y, peak area at 245 nm; x, amount (nmol) (range, 0.1–10 nmol)]; **CAR**; y = 193,581x + 6367 [y, peak area at 284 nm; x, amount (nmol)(range, 0.1–50 nmol)]; **CARQ**: y = 81,197x − 12,429 [y, peak area at 284 nm; x, amount (nmol) (range, 0.1–10 nmol)];

Analysis of the reaction products of CARQ and BCysM. To 1.8 mL CH_3CN, 63 μL of **CARQ** in CH_3CN (20 mM) and 63 μL of **BCysM** (20 mM) were added. The solution was stirred well, and 10 μL of aliquot was immediately taken from the solution and analyzed by HPLC under the following conditions: column, Cosmosil 5C18-AR-II (250 × 4.6 mm i.d, Nacalai Tesque); solvent A, acetic acid–H_2O [1:100 (v/v)]; solvent B, CH_3OH; gradient conditions, B% (time) = 60% (0 min), 100% (40 min), and 100% (40–50 min); flow rate, 0.5 mL/min; detection, 245 and 284 nm. The solution was then incubated at 35°C for 2 h, and additional aliquots were taken 1 and 2 h later and analyzed under the same conditions. The concentrations of **CARQ**, **CAR**, **BCysM**, and **(BCysM)^2** were determined using the corresponding calibration equations. New products **1** and **2** were quantitatively analyzed using the following calibration equations:**1**: y = 730,972x − 287,348 [y, peak area at 245 nm; x, amount of **1** (nmol)

(range, 0.1–20 nmol)]; **2**: y = 722,504x + 8,203 [y, peak area at 245 nm; x, amount of **2** (nmol) (range, 0.1–20 nmol)].

Preparation and structural determination of compounds 1 and 2. CH_3CN solutions (33 mL) of **CARQ** (20 mM) and **BCysM** (20 mM) were mixed well and incubated for 3 h at 37°C. The solution was evaporated to dryness, and the residue was purified by preparative HPLC [column, COSMOSIL 5C18-AR-II (250 × 20 mm i.d.); solvent, acetic acid-H_2O-CH_3OH [1:30:70 (v/v/v)]; flow rate: 10 mL/min; detection: 245 nm] to obtain **1** (25 mg) and **2** (20 mg). (Analytical data for structure determination of **1** and **2** can be found in Supporting Information)

Density functional theory (DFT) calculations. The 3D structures for the calculations were created using Avogadro (v.1.2.0)[17] and pre-optimized using molecular mechanics with the MMFF94 field from predicted stable conformers. The Gaussian (R)16 package (v.1.1; Hulinks, Tokyo, Japan)[18] was used to optimize the stereostructures and calculate the energies and natural charges of the compounds. The B3LYP method, 6-311+G(d, p) basis set, and solvation model density (SMD) [19] (solvent, CH_3CN) implemented in the package were used for the calculations.

RESULTS AND DISCUSSION

Antioxidant activity of rosemary polyphenols in the presence and absence of cysteine thiol, BCysM. The antioxidant activity of five types of rosemary polyphenols (**CA**, **CAR**, **ROS**, **epiROS**, and **isoROS**: see structures in Figure 1) was assessed by inhibiting the formation of hydroperoxides from ethyl linoleate. All polyphenols, at a concentration of 0.125 mM, showed potent antioxidant activity for up to 1 h against lipid oxidation induced by AMVN (15 mM). In contrast, the cysteine thiol **BCysM**, at the same concentration, did not display any antioxidant activity, as shown in Figure 2. Figure 2 further shows the antioxidant activity of the polyphenols with one molar equivalent of **BCysM**, revealing that only **CAR** and **isoROS** have a longer antioxidant effect in the presence of the thiol. The potent antioxidant functions of thiol compounds such as glutathione and *N*-acetylcysteine are well recognized in biological systems,[21] and their effective antioxidant activity has been observed in various assay systems, however, their efficacy depends on the radical species used, the measurement system, and other conditions.[22] In 2014, we discovered that *N*-acylcysteine esters do not exhibit antioxidant properties against lipid oxidation but cysteine derivatives with free α-amino or carboxylate groups strongly inhibit AMVN-induced linoleic acid oxidation, because of the formation of an active thiolate anion by an intramolecular proton shift to α-amino or carboxylate.[23] Comparing bond dissociation enthalpy (BDE) of S-H (ca. 86

kcal/mol) in *N*-acylcysteine esters[24] to that of hydroperoxides (OO-H, ca. 88 kcal/mol)[25] indicated that the thiol group of **BCysM** cannot exhibit effective antioxidant activity through lipid peroxyl radical trapping, but rather that degradation began with the withdrawal of a hydrogen atom at α-position with lower BDE (ca. 80 kcal/mol).[24] Thiols are also known to have high nucleophilicity and can be easily conjugate-added to carbonyl compounds. Orthoquinones are antioxidant reaction products of catechol-type polyphenols and are targets of the conjugate addition of thiols as carbonyl compounds. As a result, phenolic groups were restored, and antioxidant activity was exhibited. Several phenolic acids and flavonoids have been reported to exhibit longer antioxidant effect by this mechanism.[26–29] Figure 3 shows the results of measuring the enhancement of the antioxidant properties of **CAR** and **isoROS** by different amounts of coexisting **BCysM**; the antioxidant effect lasted longer with the amount of thiol added in both cases. Considering the structures of **CAR-** and **isoROS**-derived quinones (**CARQ** and **isoROSQ** respectively), the conjugate addition reaction of **BCysM** is only possible at one site at the 14-position. Therefore, for these diterpenoid polyphenols, other mechanisms for enhancing the antioxidant effect should be considered besides the thiol addition mechanism described.

Catalytic antioxidant properties of CAR and isoROS in the presence of BCysM.

CAR was used to elucidate the mechanism of the antioxidant reaction in the presence of **BCysM**. Figure 4 shows the results of the HPLC analysis of the antioxidant reaction products from **CAR** in the presence of one molar equivalent of **BCysM** as well as the analytical data at the beginning of the reaction. At the beginning of the reaction, the peaks of **CAR** and **BCysM** were observed at retention times 28.3 and 9.7 min respectively. During the 4-h reaction, **BCysM** decreased by 87%, while **CAR** decreased by only 22%. Three new peaks were observed at retention times 14.6, 29.8, and 31.0 min. The peak at 14.6 min was attributed to the cystine derivative **(BCysM)^2** (a dimer of **BCysM** through SS linkage) based on a comparison with the retention time of the synthetically obtained sample. Figure 5 shows the time-course change of the compounds at the peaks detected in the antioxidant reaction of **CAR** (0.63 mM) with or without **BCysM** (0.63 and 1.26 mM). Under the conditions employed (AMVN, 15 mM; ethyl linoleate, 50 mM; solvent, CH_3CN; and reaction temperature, 37°C), **CAR** decreased linearly by 68% in 4 h. However, under the same conditions, **BCysM** decreased by 44%, as shown in panels C and D respectively in Figure 4. Note that this concentration of **BCysM** did not show antioxidant activity, whereas **CAR** showed strong activity (data not shown) and produced the same amount of quinone **CARQ**. In the presence of both **CAR** and **BCysM**, the rate of decrease in **CAR** was smaller,

213 whereas that in **BCysM** was greater. Furthermore, a small amount of **CARQ** was
214 produced, while **(BCysM)^2** and new compounds **1** and **2** accumulated as the reaction
215 progressed (Figure 5, panel A). This trend was even more pronounced in the reaction of
216 **CAR** with two molar equivalents of **BCysM**, as shown in Figure 5, panel B. The
217 reaction products in the radical scavenging-antioxidation of catechol-type polyphenols
218 are *orthoquinone* derivatives.[11,30] The oxidative reactivity of **CARQ** was considered to
219 convert **BCysM** to disulfide **(BCysM)^2**. Figure 6 shows the results of HPLC analysis of
220 the reaction products from the mixture of **CARQ** and equimolar **BCysM** and from
221 **CARQ** alone and **BCysM** alone, under the same analytical conditions. The reaction
222 results showed that **CAR** and **(BCysM)^2** were formed immediately after mixing **CARQ**
223 and **BCysM**, as shown in the time course data on the right side of Figure 6. These
224 results suggest that **CARQ**, the product of the antioxidant reaction of **CAR**, is quickly
225 reduced by **BCysM** to restore **CAR** and reexhibits antioxidant activity. In conclusion,
226 **CAR** should be recognized as a catalytic antioxidant since it exhibited excellent
227 antioxidant properties in the presence of thiols in this study. **IsoROS**, which showed
228 similar antioxidant properties, could be another catalytic antioxidant. Antioxidant
229 catalysts have been examined by several studies. They are mimics of the catalytic sites
230 of redox enzymes[31] or synthetic compounds containing heavy chalcogen atoms with

high redox reactivity.[32] This study is the first to report the catalytic antioxidant activity of diterpenoid polyphenols **CAR** and **isoROS**, but not of **CA**, **ROS**, and **epiROS**.

The addition products of BCysM to CARQ. Thiols have high nucleophilic activity and can undergo conjugate addition to quinones. This addition reaction is another mechanism whereby the antioxidant activity of polyphenols can be enhanced by restoring the 1,2-diphenol structure.[27,28,33] In the reaction of **CARQ** with **BCysM**, the same products **1** and **2** from the antioxidant reaction of **CAR** were detected, as shown in Figures 4 and 6. Compounds **1** and **2** were successfully isolated from the reaction mixture of **CARQ** and **BCysM**. The HR-MS data of **2** revealed its molecular formula to be $C_{31}H_{37}NO_7S$ (*m/z* 566.2198 $[M-H]^-$). The ^{1}H-NMR data of **2** showed signal sets similar to those of **CAR** and **BCysM,** but did not show signals corresponding to the proton at the 14-position of **CAR** and the thiol group of **BCysM**. These data revealed that **2** was a coupling product of **CAR** and **BCysM** between the 14-position of **CAR** and the thiol group of **BCysM**, as shown as structure 2 in Figure 7. The molecular formula of compound **1** was estimated to be $C_{31}H_{35}NO_7S$ from its HR-MS data (*m/z* 564.2042 $[M-H]^-$). ^{1}H-NMR data of **1** showed similar data to those of **2**, indicating the same coupling structure with **CAR** and **BCysM**. However, two protons were missing from the proton set owing to **BCysM**, and a low-field-shifted olefinic proton was

observed at 7.14 ppm. These data indicated that **1** was an oxidized compound at the 1′,2′-positions of the **BCysM** part. The stereostructure of the olefin was determined to be *Z* by observing the nuclear Overhauser effect (NOE) from 3′-OCH_3 to H-1′. Thus, the structure of **1** was determined to be a dehydrocysteine-substituted **CAR** as shown in Figure 7. Both compounds were addition products of the thiol to the 14-position of **CARQ** and have restored diphenol groups, which again exhibit antioxidant activity. Although the reason for the production of oxidized product **1** is unclear, radical oxidation may occur at the α-position of **BCysM**, where the bond dissociation enthalpy of the carbon-proton bond is lowest, producing a 1,2-dehydro derivative of **BCysM**, which may act as another nucleophilic thiol.

Prediction of the reaction mechanisms of rosemary polyphenol quinones with BCysM based on DFT calculations Quinones are known to have both oxidative and electrophilic addition reactivities, and thiols have reductive and nucleophilic addition reactivities, which shape their functional expression in foods and living cells.[34] Regardless of the type of reactions, both reactivities of substituted quinones generally increase with the electron-withdrawing capacity of the substituent groups.[35,36] In the studied polyphenols, the only differing substituent attached to the quinone structure is the alkyl group adjacent to the 8-position. Specifically, **CA** has a simple methylene

group, **ROS** and **epiROS** have a hydroxymethylene group, and **CAR** and **isoCAR** have an acyloxymethylene group, as shown in Figure 1. The most electron-withdrawing group is the acyloxymethylene group, which explains the high reactivity of the quinone derivatives of **CAR** and **isoROS** (**CARQ** and **isoROSQ** respectively) with the thiol compound **BCysM**. These considerations, based on the electronic theory of classical organic chemistry, were confirmed by *ab initio* calculations. Table 1 shows the DFT calculation results for the following redox reaction between **BCysM** and the quinone derivatives of rosemary polyphenols.

Polyphenol quinone + 2 **BCysM** ⇄ Polyphenol + **(BCysM)$_2$**

(Optimized stereostructures resulting from the calculations are shown in Figure S1). Compared with other polyphenol quinones, the larger negative values (−7.405 and −6.338 kcal/mol respectively) of the calculated Gibbs free energy change (ΔG) in the reactions of **isoROSQ** and **CARQ** indicate that the reactions yield the products more efficiently. Although a comparison of transition states is necessary to accurately determine reaction rates, if the Bell-Evans-Polany principle[37] or Marcus theory[38] can be adapted, the high negative ΔG values of **isoROS** and **CAR** would suggest that these reactions occurred more rapidly.

Quinones have multiple reaction positions for nucleophilic addition and have a high potential for redox reactions, therefore, the predicting the reaction mechanism is challenging. Although many methods have been developed to predict reactive positions,[39] in this study, the most reactive position of **CARQ** and predicted intermediates was selected based on the condensed Fukui function, easily obtained by the natural population analysis of DFT calculations.[40] The indices for the condensed Fukui functions were obtained using UCA-FUKUI software.[41] The values for the atoms of orthoquinone moieties of **CARQ** and its reaction intermediates are summarized in Table 2. As for the ionic reaction mechanism (Scheme 1 in Figure 8), the most reactive position in the nucleophilic attack on **CARQ** is the 8-position (f^+ = 0.216), where **BCysM** reacts nucleophilically to form intermediate **3**. Although the 14-positon is the third most reactive position of **3** for nucleophilic attack (f^+ = 0.139), the electrophilic reactivity of S at the 8-position is predominant (f^- = 0.335) in comparison with other positions. Therefore, intramolecular cyclization may occur to yield **4**. The thiol anion produced in the reaction thus far makes a nucleophilic attack on the thiirane S atom (f^+ = 0.589) at the 8- and 14-positions, resulting in the formation of **CAR** and disulfide **(BCysM)^2**. Reacting at the second reactive 14-position (f^0 = 0.107) of **4**, the thiirane ring is opened by the attack of the thiyl anion (RS^-), and the aromaticity is

302 restored by the elimination of one mole of the thiol to yield product **2**. In the hydrogen
303 atom transfer and radical reaction mechanism (Scheme 2 in Figure 8), the most
304 radically reactive carbonyl oxygen ($f^0 = 0.123$) at the 11-position of **CAR** is attacked
305 by an hydrogen atom from **BCysM** to form the 11-radical of semiquinone **5** and the
306 thiyl radical (RS•). The most radically reactive carbonyl oxygen ($f^0 = 0.191$) at the 12-
307 carbonyl group of **5**, further absorbs a hydrogen atom from another **BCysM**. The two
308 thiyl radicals produced couple to form disulfide **(BCysM)^2**. These successive reactions
309 correspond to the redox reactions of **CARQ** and **BCysM**. When the thiyl radical reacts
310 at the second reactive 8-position of **5**, the same product **3** is formed as the product of
311 the ionic reaction scheme, and the subsequent ionic reaction pathway produces **CAR**
312 and **2**.

313 In conclusion, **CAR** and **isoROS** in rosemary diterpenoid polyphenols showed
314 catalytic antioxidant activity in the presence of thiols. This mechanism allows **CAR**
315 and **isoROS** to continuously exhibit antioxidant properties in the presence of thiol-
316 containing substances as long as thiols are present. Antioxidant activity depends on the
317 physicochemical properties of the antioxidant used. The use of catalytic antioxidants is
318 advantageous in that their superior properties are continuously maintained during food
319 storage. Further, two quinone derivatives, the antioxidant products of **CAR** and

isoROS, were found to efficiently convert thiols to disulfides. Quinone substances are well known to be toxic to living organisms. This toxicity is attributed to the irreversible binding of quinones to biomaterials including protein thiol.[42] Therefore, the mechanism of thiol addition to quinones has been extensively studied.[43] On the other hand, the mechanism of disulfide formation by quinones is complex and not yet fully understood.[44] Importantly, this reaction has the advantage of yielding only the original polyphenol and disulfide without producing toxic substances. Furthermore, the formation of disulfide bonds is important for improving the texture of food products, such as in the dough formation of flour[45] and the texture improvement of meat.[46] Therefore, quinone derivatives of **CAR** and **isoROS** could be utilized as texture modifiers in food processing, because they preferentially form disulfides over addition products.

ASSOCIATED CONTENT

Supporting Information

Supporting information is available free of charge.

1. Analytical Data for Identification of **isoROS**, **ROS**, and **epiROS**.

2. Analytical Data for Structure Determination of Compounds **1** and **2**.

338 3. Figure S1. Drawing of the Optimized Stereostrucures of Rosemary Polyphenols,

339 Their Quinone Derivatives, **BCysM**, and **(BCysM)^2**.

340

341 ACKNOWLEDGMENT

342 We thank Dr. Hiromi Hayashida of Mitsubishi Chemical Corporation for providing the

343 rosemary extract and Ms. Kayo Hidaka for her assistance with DFT calculations.

344

345 AUTHOR INFORMATION

346 **Corresponding Author**

347 **Toshiya Masuda** – *Graduate School of Human Life Science, Osaka Metropolitan*

348 *University, Osaka 558-8585, Japan;* orciid.org/ 0000-0001-6691-9464;

349 Email: tmasuda@omu.ac.jp

350 **Authors**

351 **Hayate Higashino** – *Graduate School of Human Life Science, Osaka Metropolitan*

352 *University, Osaka 558-8585, Japan;*

353 Email: si22826d@st.omu.ac.jp

354 **Asuka Karatsu** – *Graduate School of Human Life Science, Osaka Metropolitan*

355 *University, Osaka 558-8585, Japan;*

Email: hornfels1215@gmail.com

Authors Contributions

T. M. did the study conceptualization. H. H. performed the experiments, data analysis, and DFT calculations. A. K. performed the experiments. All authors have approved the final version of the manuscript for submission.

Founding

This study was supported by JSPS KAKENHI (Grant Number 23H00912).

Notes

The authors declare no competing financial interests.

366 REFERENCES

367 (1) Frankel, E. N. The problems of using one-dimensional methods to evaluate
368 multifunctional food and biological antioxidants, *J. Sci. Food Agric.* **2000**, *80*, 1925–
369 1941.

370 (2) Shahidi, F.; Zhong, Y. Revisiting the polar paradox theory: A critical overview. *J.*
371 *Agric. Food Chem.* **2011**, *59*, 3499–3504.

372 (3) Olszowy-Tomezyl, M. Synergistic, antagonistic and additive antioxidant effects in
373 the binary mixture, *Phytochem. Rev.* **2020**, *19*, 63–103.

374 (4) Bayram, I.; Decker, E. A. Underlyng mechanism of synergistic antioxidant
375 interactions during lipid oxidation. *Trends Food Sci. Technol.* **2023**, *133*, 219-230.

376 (5) Cuppett, S. L.; Hall, C. A. Antioxidant activity of the Labiatae. *Adv. Food Nutr.*
377 *Res.* **1998**, *42*, 245–272.

378 (6) Aruoma, O. I.; Halliwell, B.; Aeschbach, R.; Löligers, J. Antioxidant and pro-
379 oxidant properties of active rosemary constituents: carnosol and carnosic acid.
380 *Xenobiotica* **1992**, *22*, 257–268.

381 (7) Hraš, A. R.; Hadolin, M.; Knez, Ž.; Bauman, D. Comparison of antioxidative and
382 synergistic effects of rosemary extract with α-tocopherol, ascorbyl palmitate and citric
383 acid in sunflower oil. *Food Chemistry* **2000**, *71*, 229–233.

(8) Terao, J.; Matsushita, S. In *Kasanka Shishitsu Jikkenhou (Lipid peroxide experimental methods)*; Kaneda, T.; Ueta, N. Eds. Ishiyaku: Tokyo, 1983; pp 22–35.

(9) Terao, J.; Matsushita, S. Products formed by photosensitized oxidation of unsaturated fatty acid esters. *J. Am. Oil Chem. Soc.* **1977**, *54*, 234–238.

(10) Fujimoto, A.; Masuda, T. Chemical interaction between polyphenols and a cysteinyl thiol under radical oxidation conditions. *J. Agric. Food Chem.* **2012**, *60*, 5142–5151.

(11) Masuda, T.; Inaba, Y.; Takeda, Y. Antioxidant mechanism of carnosic acid: structural identification of two oxidation products. *J. Agric. Food Chem.* **2001**, *49*, 5560–5565.

(12) Masuda, T.; Kirikihira, T.; Takeda, Y.; Yonemori, S. Thermal recovery of antioxidant activity from carnosol quinone, the main antioxidation product of carnosol. *J. Sci. Food Agric.* **2004**, *84*, 1421–1427.

(13) Patiny, L.; Borel, A. ChemCalc: A building block for tomorrow's chemical infrastructure. *J. Chem. Inf. Model.* **2013**, *53*, 1223–1228. (https://www.chemcalc.org)

(14) Nakatani, N.; Inatani, R. (1981). Structure of rosmanol, a new antioxidant from rosemary (*Rosmarinus officinalis* L.). *Agric. Biol. Chem.* **1981**, *45*, 2385–2386.

(15) Nakatani, N.; Inatani, R. (1984). Two antioxidative diterpenes from rosemary

(*Rosmarinus officinalis* L.) and a revised structure for rosmanol. *Agric. Biol. Chem.* **1984**, *48*, 2081–2085.

(16) Cuvelier, M. E.; Berset, C.; Richard, H. Antioxidant constituents in sage (*Salvia officinalis*). *J. Agric. Food Chem.* **1994**, *42*, 665–669.

(17) Hanwell, M. D.; Curtis, D. E.; Lonie, D. C.; Vandermeersch, T.; Zurek, E.; Hutchison, G. R. Avogadro: an advanced semantic chemical editor, visualization, and analysis platform. *J. Cheminformatics* **2012**, *4*, 1–17.

(18) Frisch, M. J.; Trucks, G. W.; Schlegel, H. B.; Scuseria, G. E.; Robb, M. A.; Cheeseman,J. R.; Scalmani, G.; Barone, V.; Petersson, G. A.; Nakatsuji, H.; Li, X.; Caricato, M.; Marenich, A. V.; Bloino, J.; Janesko, B. G.; Gomperts, R.; Mennucci, B.; Hratchian, H. P.; Ortiz, J. V.; Izmaylov, A. F.; Sonnenberg, J. L.; Williams-Young, D.; Ding, F.; Lipparini, F.; Egidi, F.; Goings, J.; Peng, B.; Petrone, A.; Henderson, T.; Ranasinghe, D.; Zakrzewski, V. G.; Gao, J.; Rega, N.; Zheng, G.; Liang, W.; Hada, M.; Ehara, M.; Toyota, K.; Fukuda, R.; Hasegawa, J.; Ishida, M.; Nakajima, T.; Honda, Y.; Kitao, O.; Nakai, H.; Vreven, T.; Throssell, K.; Montgomery Jr., J. A.; Peralta, J. E.; Ogliaro, F.; Bearpark, M. J.; Heyd, J. J.; Brothers, E. N.; Kudin, K. N.; Staroverov, V. N.; Keith, T. A.; Kobayashi, R.; Normand, J.; Raghavachari, K.; Rendell, A. P.; Burant, J. C.; Iyengar, S. S.; Tomasi, J.; Cossi, M.; Millam, J. M.; Klene, M.; Adamo, C.;

Cammi, R.; Ochterski, J. W.; Martin, R. L.; Morokuma, K.; Farkas, O.; Foresman, J. B.; Fox, D. J. Gaussian 16 Rev. C.01/C.02, Gaussian, Inc., Wallingford CT, 2016.

(19) Marenich, A. V.; Cramer, C. J.; Truhlar, D. G. Universal solvation model based on solute electron density and on a continuum model of the solvent defined by the bulk dielectric constant and atomic surface tensions. *J. Phys. Chem. B* **2009**, *113*, 6378–639.

(20) Jónsson, H.; Mills, G.; Jacobsen, K. W. Nudged elastic band method for finding minimum energy paths of transitions. In *Classical and quantum dynamics in condensed phase simulations.* Berne, B. J.; Ciccotti, G.; Coker, D. F. Eds. World Scientific: Singapore, 1998, pp 385–404.

(21) Deneke, S. M. Thiol-based antioxidants. *Current Topics in Cellular Regulation* **2001**, *36*, 151–180.

(22) Apak, R.; Özyürek, M.; Güçlü, K.; Çapanoğlu, E. Antioxidant activity/capacity measurement. 1. Classification, physicochemical principles, mechanisms, and electron transfer (ET)-based assays. *J. Agric. Food Chem*. **2016**, *64*, 997–1027.

(23) Miura, Y.; Honda, S.; Masuda, A.; Masuda, T. Antioxidant activities of cysteine derivatives against lipid oxidation in anhydrous media. *Biosci. Biotechnol. Biochem.* **2014**, *78*, 1452–1455.

(24) Haya, L.; Mainar, A. M.; Pardo, J. I.; Urieta, J. S. A new generation of cysteine

derivatives with three active antioxidant centers: improving reactivity and stability. *Phys. Chem. Chem. Phys.* **2014**, *16*, 1409–1414.

(25) Košinová, P.; Di Meo, F.; Anouar, E. H.; Duroux, J. L.; Trouillas, P. (2011). H-atom acceptor capacity of free radicals used in antioxidant measurements. *Int. J. Quantum Chem.* **2011**, *111*, 1131–1142.

(26) Saito, S.; Kawabata, J. Synergistic effects of thiols and amines on antiradical efficiency of protocatechuic acid. *J. Agric. Food Chem.* **2004**, *52*, 8163–8168.

(27) Bassil, D.; Makris, D. P.; Kefalas, P. Oxidation of caffeic acid in the presence of L-cysteine: isolation of 2-S-cysteinylcaffeic acid and evaluation of its antioxidant properties. *Food Res. Int.* **2005**, *38*, 395–402.

(28) Fujimoto, A.; Inai, M.; Masuda, T. Chemical evidence for the synergistic effect of a cysteinyl thiol on the antioxidant activity of caffeic and dihydrocaffeic esters. *Food Chemistry* **2013**, *138*, 1483–1492.

(29) Masuda, T.; Miura, Y.; Inai, M.; Masuda, A. Enhancing effect of a cysteinyl thiol on the antioxidant activity of flavonoids and identification of the antioxidative thiol adducts of myricetin. *Biosci. Biotechnol. Biochem.* **2013**, *77*, 1753–1758.

(30) Kawabata, J.; Okamoto, Y.; Kodama, A.; Makimoto, T.; Kasai, T. (2002). Oxidative dimers produced from protocatechuic and gallic esters in the DPPH radical

scavenging reaction. *J. Agric. Food Chem.* **2002,** *50*, 5468–5471.

(31) Day, B. J. Antioxidants as potential therapeutics for lung fibrosis. *Antioxid. Redox Signal.* **2008**, 10, 355–370.

(32) Ingold, K. U.; Pratt, D. A. Advances in radical-trapping antioxidant chemistry in the 21st century: a kinetics and mechanisms perspective. *Chem. Rev.* **2014**, 114, 9022–9046.

(33) Liang, Y.; Were, L. Cysteine's effects on chlorogenic acid quinone induced greening and browning: Mechanism and effect on antioxidant reducing capacity. *Food Chemistry* **2020**, *309*, 125697.

(34) Brunmark, A.; Cadenas, E. Redox and addition chemistry of quinoid compounds and its biological implications. *Free Radic. Biol. Med.* **1989**, *7*, 435–477.

(35) Frontana, C.; Vázquez-Mayagoitia, Á.; Garza, J.; Vargas, R.; González, I. Substituent effect on a family of quinones in aprotic solvents: an experimental and theoretical approach. *J. Phys. Chem. A* **2006**, *110*, 9411–9419.

(36) Guo, X.; Mayr, H. Quantification of the ambident electrophilicities of halogen-substituted quinones. *J. Am. Chem. Soc.* **2014**, *136*, 11499–11512.

(37) Mayr, H.; Ofial, A. R. The reactivity–selectivity principle: an imperishable myth in organic chemistry. *Angew. Chem. Int. Ed.* **2006**, *45*, 1844–1854.

(38) Albery, W. J. The application of the Marcus relation to reactions in solution. *Annu. Rev. Phys. Chem.* **1980**, 31, 227–263.

(39) Wang, B.; Rong, C.; Chattaraj, P. K.; Liu, S. A comparative study to predict regioselectivity, electrophilicity and nucleophilicity with Fukui function and Hirshfeld charge. *Theor. Chem. Acc.* **2019**, *138*, 1–9.

(40) Wang, L.; Ding, J.; Pan, L.; Cao, D.; Jiang, H.; Ding, X. Quantum chemical descriptors in quantitative structure–activity relationship models and their applications. *Chemometr. Intell. Lab. Syst.* **2021**, *217*, 104384.

(41) Sánchez-Márquez, J.; Zorrilla, D.; Sánchez-Coronilla, A.; de los Santos, D. M.; Navas, J.; Fernández-Lorenzo, C.; Alcántara, R.; Martín-Calleja, J. Introducing "UCA-FUKUI" software: reactivity-index calculations. *J. Mol. Model.* **2014**, *20*, 2492.

(42) Bolton, J. L.; Trush, M. A.; Penning, T. M.; Dryhurst, G.; Monks, T. J. (2000). Role of quinones in toxicology. *Chem. Res. Toxicol.* **2000**, *13*, 135–160.

(43) Alfieri, M. L.; Cariola, A.; Panzella, L.; Napolitano, A.; d'Ischia, M.; Valgimigli, L.; Crescenzi, O. Disentangling the puzzling regiochemistry of thiol addition to o-quinones. *J. Org. Chem.* **2022**, *87*, 4580–4589.

(44) Bader, M. W.; Xie, T.; Yu, C. A.; Bardwell, J. C. Disulfide bonds are generated by quinone reduction. *J. Biol. Chem.* **2000**, *275*, 26082–26088.

(45) Joye, I. J.; Lagrain, B.; Delcour, J. A. Endogenous redox agents and enzymes that affect protein network formation during breadmaking–A review. *J. Cereal Sci.* **2009**, *50*, 1–10.

(46) Bao, Y.; Ertbjerg, P. Effects of protein oxidation on the texture and water-holding of meat: A review. *Crit. Rev. Food Sci. Nutri.* **2019**, *59*, 3564–3578.

Table 1. Calculated Gibbs Free Energy Change of the Reaction of Rosemary Polyphenol Quinones and BCysM.

Compound	*Δ*G (kcal/mol)
isoROSQ	−7.405
CARQ	−6.338
epiROSQ	−4.895
ROSQ	−4.518
CAQ	−2.824

*Δ*G was calculated by the equation: ΔG = [G(Quinone) + G(**(BzCysM)^2**)] − [G(Polyphenol) + G(**BzCysM**) × 2]. G is the sum of electronic and thermal free energy calculated by DFT method using B3LYP functional, 6-311+G(d,p) basis set, and SMD solvation model (CH_3CN).

Table 2. Condensed Fukui Indices of the Atoms in Quinone Moieties of CARQ and Its Predicted Intermediates for Nucleophilic (f^+), Electrophilic (f^-), and Radical (f^0) Attacks.

	CARQ		3		4	5
Atom position	f^+	f^0	f^+	f^-	f^+	f^0
C-8	**0.216**	0.080	−0.046	0.013	−0.108	0.167
C-9	−0.014	0.108	0.136	0.055	0.001	0.066
C-11	0.128	0.060	−0.008	0.074	0.023	0.090
C-12	0.139	0.065	**0.207**	−0.027	0.052	0.080
C-13	0.041	0.110	0.017	0.092	0.001	0.116
C-14	0.046	0.081	0.139	0.031	0.107	0.016
11-C-O	0.156	**0.123**	0.029	0.069	0.000	0.080
12-C-O	0.156	0.117	0.170	0.027	0.023	**0.191**
8-C-S or 8,14-C-S	-	-	0.130	**0.335**	**0.589**	-

The Fukui index (f^+ for nucleophilic attack, f^- for electrophilic attack, and f^0 for radical attack) values were obtained using UCA-FUKUI software through the finite difference approximation using the natural charges of corresponding atoms, which were obtained by DFT calculations. Bold number in each column indicates the largest Fukui index value.

Methyl mercaptan (CH_3SH) was used as the thiol for DFT calculations instead of **BCysM**.

525

526

527 **Figure captions**

528 **Figure 1.** Chemical structures of five rosemary polyphenols and *N*-benzyolcysteine

529 methyl ester (**BCysM**).

530

531 **Figure 2.** Antioxidant activity of rosemary polyphenols in the presence or absent of

532 **BCysM**.

533 Reaction conditions: Ethyl linoleate, 50 mM; AMVNN, 15 mM; Polyphenols, 0.125

534 mM; and **BCysM**, 0.125 mM in CH_3CN at 37°C. Data are presented by mean ± SE (n =

535 2).

536

537 **Figure 3.** Concentration effects of **BCysM** on antioxidant activity of **CAR** and **isoROS**.

538 Reaction conditions: Ethyl linoleate, 50 mM; AMVNN, 15 mM; Polyphenols, 0.125

539 mM; and **BCysM**, 0.125–0.375 mM in CH_3CN at 37°C. Data are presented by mean ±

540 SE (n = 2).

541

542 **Figure 4.** HPLC analytical results of antioxidant reaction solutions of **CAR** in the

543 presence of **BCysM**.

Reaction conditions: Ethyl linoleate, 50 mM; AMVNN, 15 mM; **CAR**, 0.63 mM; and **BCysM**, 0.63 mM in CH_3CN at 37°C. Analytical conditions: column, Cosmosil 5C18-AR-II (250 × 4.6 mm i.d); solvent A, acetic acid–H_2O (1:100); solvent B, CH_3OH; gradient conditions, B% (time) = 60% (0 min), 100% (40 min), 100% (40–50 min); and flow rate, 0.5 mL/min.

Figure 5. Quantitative time-course data for **CAR**, **CARQ**, **BCysM**, **(BCysM)^2**, and compounds **1** and **2** in antioxidant reaction solutions.

Panel A: Reaction of **CAR** (0.63 mM) and **BCysM** (0.63 m); Panel B: Reaction of **CAR** (0.63 mM) and **BCysM** (1.26 mM); Panel C: Reaction of **CAR** (0.63 mM); Panel D: Reaction of **BCysM** (0.63 mM). Other reaction conditions: Ethyl linoleate, 50 mM; AMVNN, 15 mM in CH_3CN at 37°C.

Figure 6. HPLC analysis data for **CARQ**, **BCysM** and a reaction mixture of **CARQ** and **BCysM**, and time-course data for the reaction mixture.

Reaction conditions: 0.63 mM CARQ and 0.63 mM **BCysM** in CH_3CN at 37°C Analytical conditions: column, Cosmosil 5C18-AR-II (250 × 4.6 mm i.d); solvent A, acetic acid–H_2O (1:100); solvent B, CH_3OH; gradient conditions, B% (time) = 60% (0

562 min), 100% (40 min), and 100% (40–50 min); and flow rate, 0.5 mL/min.

563

564 **Figure 7.** Chemical structures of compounds **1** and **2**.

565 Position numbers were tentatively assigned based on those of abietane diterpenoids.

566

567 **Figure 8.** Reaction mechanisms of **CARQ** and thiol based on the condensed Fukui

568 indices.

569 RS-H = **BCysM**, RSSR = **(BCysM)^2**. Calculations were performed using methyl

570 mercaptan (CH_3SH) as the thiol instead of **BCysM**.

571 Scheme 1. Mechanism starting from the nucleophilic addition of RSH to **CARQ**,

572 followed by intramolecular addition and second nucleophilic addition or isomerization.

573 Scheme 2. Mechanism staring from the hydrogen atom transfer reaction from RSH

574 to **CARQ**, followed by radical coupling and intramolecular addition (the same

575 nucleophilic addition or isomerization as shown in Scheme 1).

576

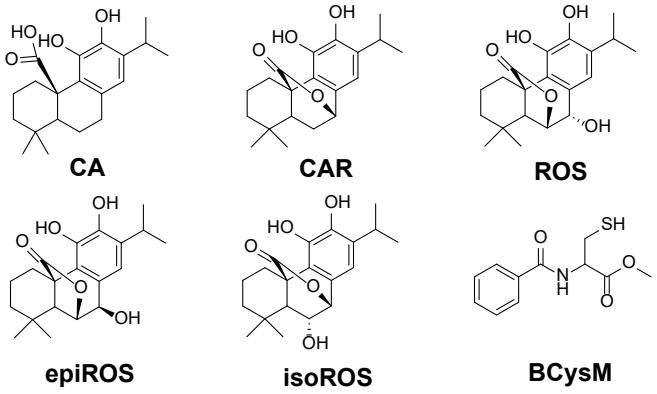

577

578 **Fig. 1**

579

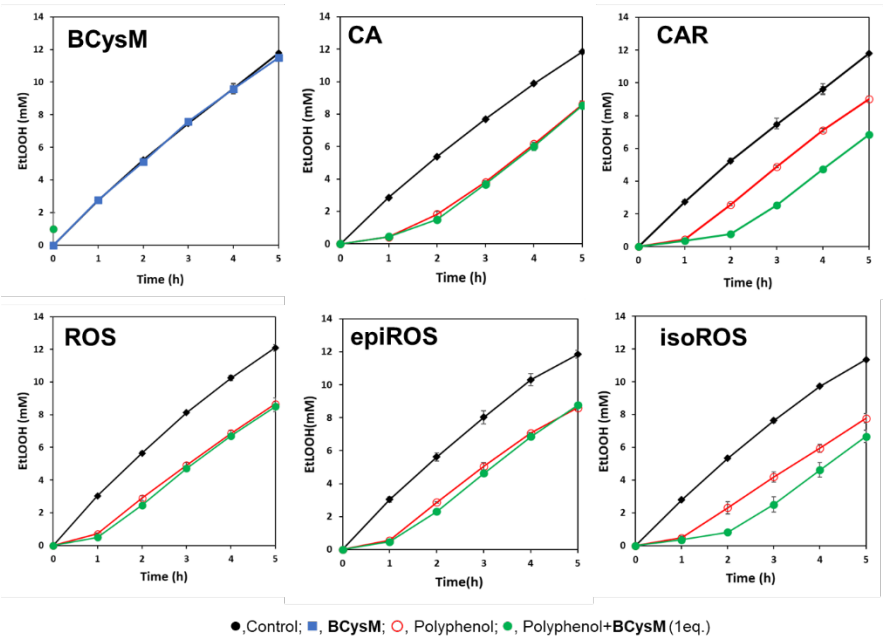

580

581 **Fig. 2**

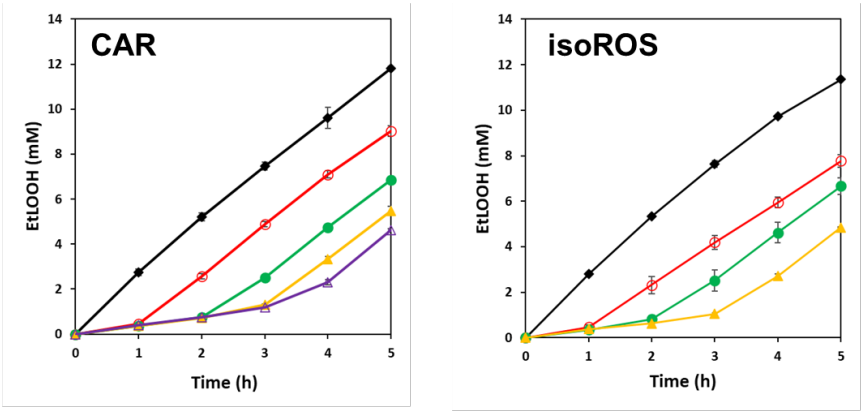

582

583 **Fig. 3**

584

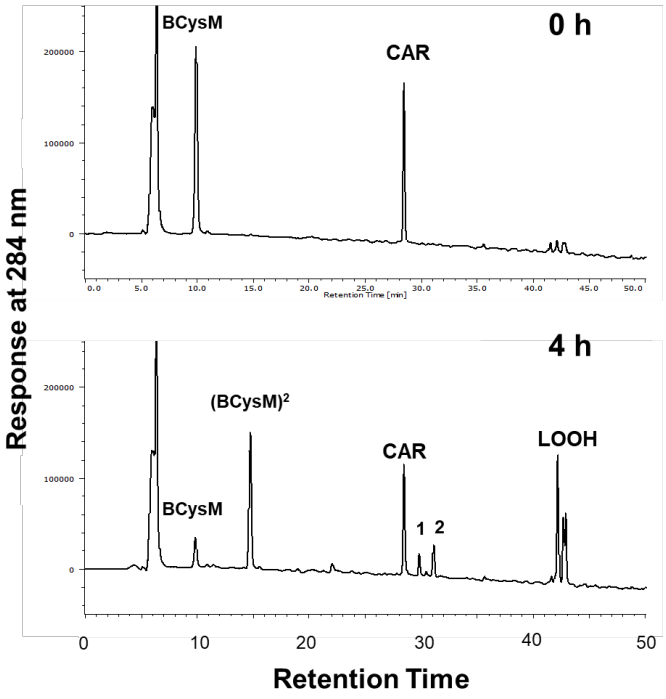

585

586 **Fig. 4**

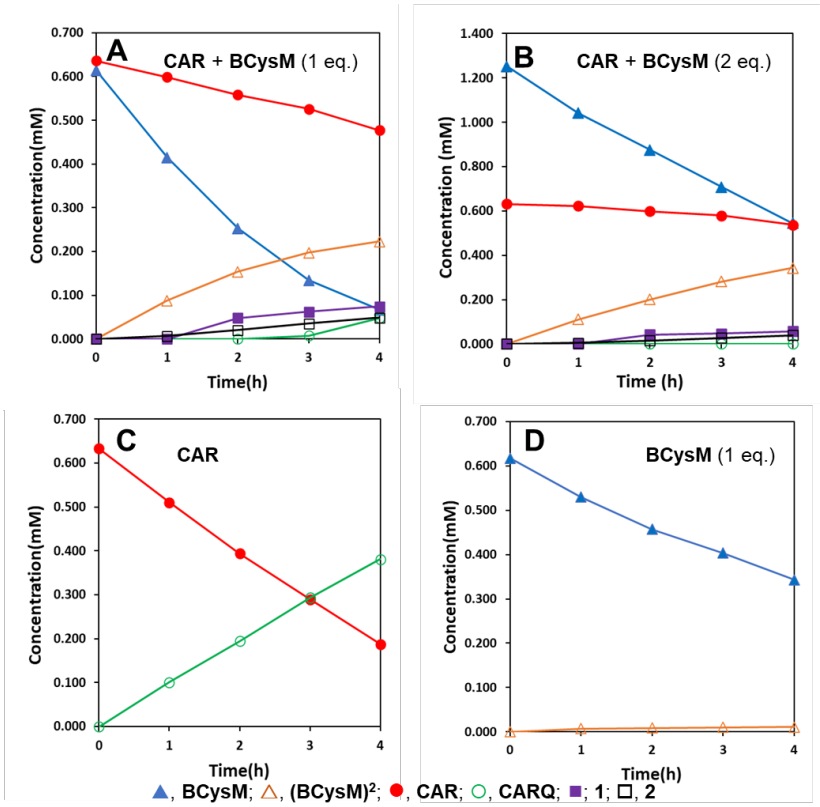

587

588 **Fig. 5**

589

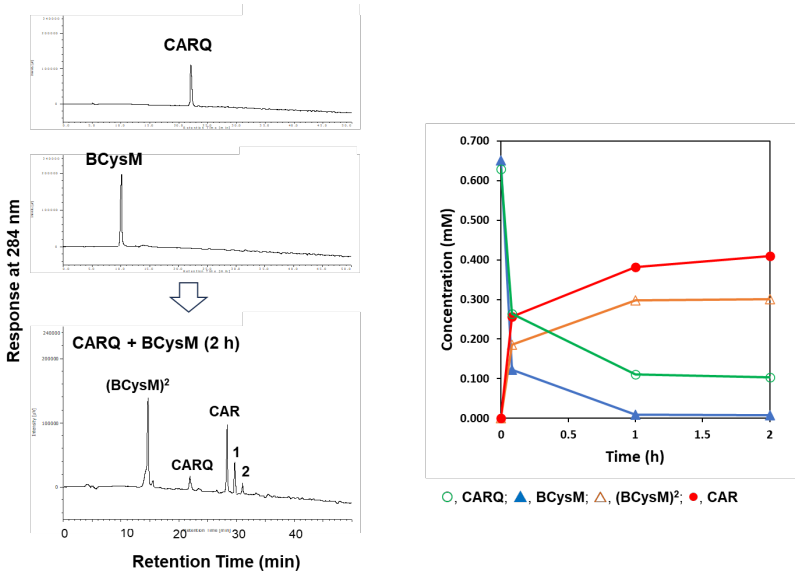

590

591 **Fig. 6**

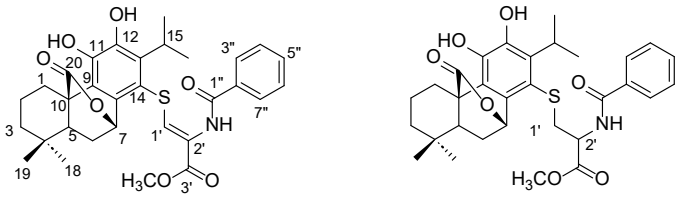

1 **2**

592

593 **Fig. 7**

594

Scheme 1. Ionic Reaction Mechanism

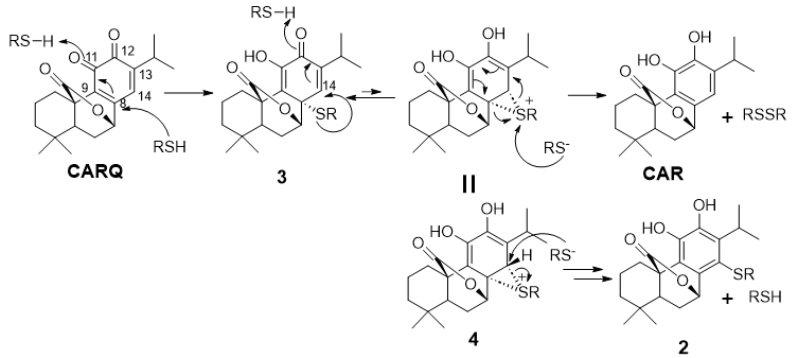

Scheme 2. Hydrogen Atom Transfer–Radical Reaction Mechanism

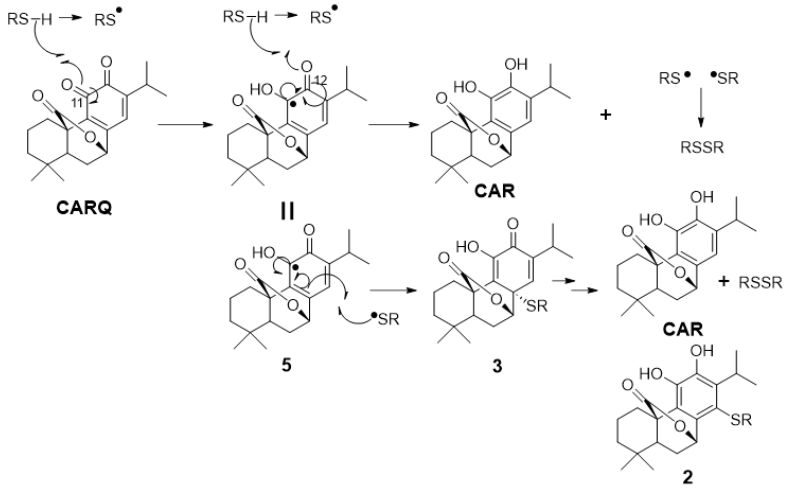

595

596

597 **Fig. 8**

598

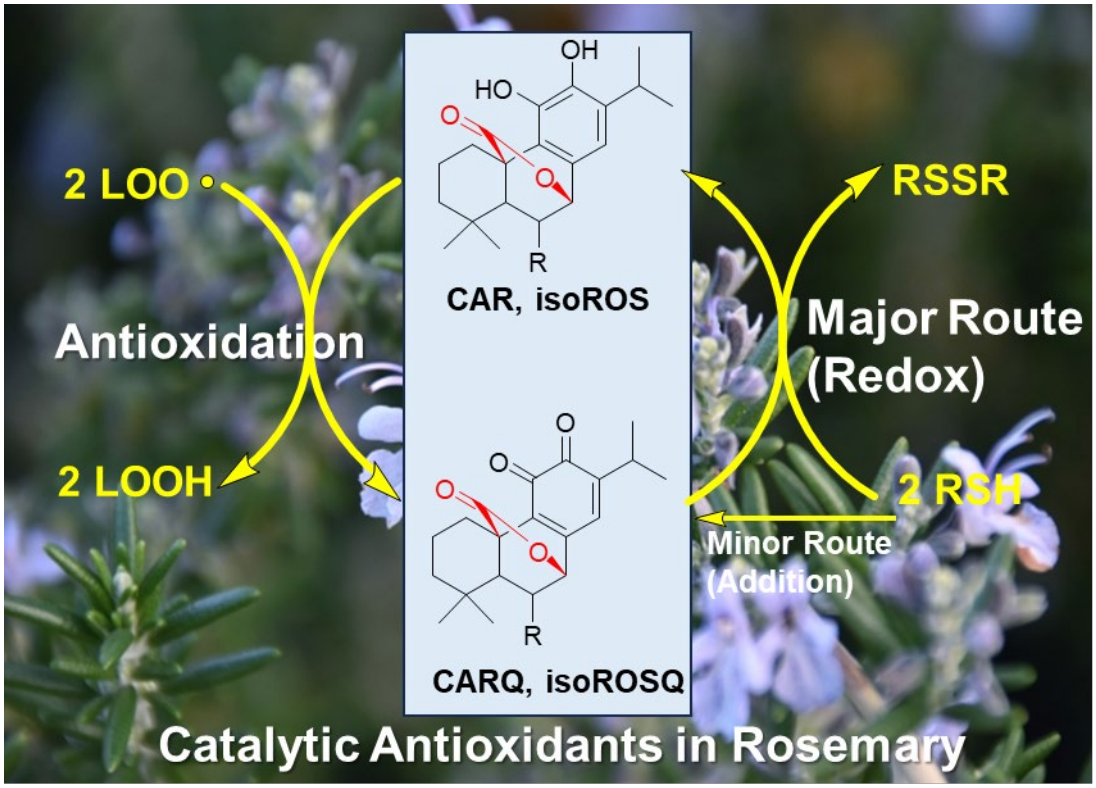

TOC Graphic Abstract